remote sensing

MDPI

Article

Exploring the Relationship between the Eco-Environmental Quality and Urbanization by Utilizing Sentinel and Landsat Data: A Case Study of the Yellow River Basin

Xiaolei Wang [1,2,*], Shiru Zhang [1], Xue Zhao [1], Shouhai Shi [1] and Lei Xu [3]

1 The School of Geoscience and Technology, Zhengzhou University, Zhengzhou 450052, China
2 Joint Laboratory of Eco-Meteorology, Zhengzhou University, Chinese Academy of Meteorological Sciences, Zhengzhou University, Zhengzhou 450052, China
3 National Engineering Research Center for Geographic Information System, School of Geography and Information Engineering, China University of Geosciences (Wuhan), Wuhan 430074, China
* Correspondence: xiaolei8788@zzu.edu.cn

Abstract: Yellow River Basin urban agglomeration (YRBU) is the main carrier of regional socio-economic development in the Yellow River Basin, and its eco-environmental quality, urbanization, and coupling coordination degree are facing higher demands. It is of great significance for the development of YRBU to understand the interactive coupling relationship between the eco-environment and urbanization development from the multi-scale perspective. This research intended to understand the spatio-temporal characteristics of eco-environmental quality, urbanization, and coupling coordination degree in the study area from 2013 to 2021. We proposed an Adjusted Remote Sensing Ecological Index (A-RSEI), integrated Sentinel-2A, Landsat 8, and other remote sensing data to evaluate the eco-environmental quality of the study area, from 2013 to 2021. Coupled coordination degree (CCD) model was used to obtain the CCD between eco-environmental quality and urbanization. In addition, spatio-temporal and multi-scale analysis was carried out from the perspectives of urban agglomeration, municipal, county, and pixel scales. Combined with spatial autocorrelation analysis and Tapio decoupling model, the CCD was further explored. The results show that the proposed A-RSEI model is more suitable for monitoring the eco-environmental quality of the Yellow River Basin. The coupling coordination degree of eco-environment and urbanization in most regions of the study area are rising in a relatively green development trend. The multi-scale analysis among eco-environmental quality, urbanization, and CCD can not only indicate the impact of the central city on its surrounding areas but also help to describe the details of CCD combined with the terrain. The comprehensive discrimination of urban agglomeration and county scale is helpful to express the relationship between urbanization and eco-environmental quality centered on a certain city. The results can provide scientific support for eco-environment protection and high-quality development of the Yellow River Basin.

Keywords: eco-environmental quality; urbanization; coupling coordination degree; Yellow River Basin; urban agglomeration

Citation: Wang, X.; Zhang, S.; Zhao, X.; Shi, S.; Xu, L. Exploring the Relationship between the Eco-Environmental Quality and Urbanization by Utilizing Sentinel and Landsat Data: A Case Study of the Yellow River Basin. *Remote Sens.* **2023**, *15*, 743. https://doi.org/10.3390/rs15030743

Academic Editors: Xiaonan Tai, Xiang Zhang and Peng Fu

Received: 30 November 2022
Revised: 16 January 2023
Accepted: 24 January 2023
Published: 27 January 2023

1. Introduction

Ecological protection in the Yellow River Basin plays an important role in the construction of the ecological barrier in northern China [1]. However, with the development of economic construction and urbanization, there are problems such as resource consumption and environmental pollution. As the main carrier of regional socio-economic development in the Yellow River Basin [2,3], the development of eco-environmental quality in urban agglomerations is closely related to its rapid urbanization [4,5]. The Comprehensive Plan for the Yellow River Basin [6], the need for ecological protection and high-quality development, has set higher requirements for the eco-environmental quality, urbanization development, and coupling coordination degree of the study area. Therefore, the spatio-temporal evolution of eco-environmental quality and the coupling relationship between urbanization and eco-environmental quality is conducive to the sustainable ecological development of the Yellow River Basin.

With the rapid development of remote sensing technology and the open access of multi-source remote sensing data, the related method for assessing eco-environmental quality and urbanization have been promoted [7–9]. Among them, in the urbanization evaluation study, for example, night light data can be used to capture stable light source information in urban areas and directly reflect the intensity of social and economic activities [10,11], and remote sensing image data can be used to extract built-up areas and reflect land use changes [12].

In the evaluation of eco-environmental quality, Xu et al. [13] proposed a remote sensing ecological index (RSEI) based on remote sensing data, in 2013, by integrating greenness, dryness, humidity, and heat indicators. The model has been widely used in regional eco-environmental quality monitoring [14–18], such as the assessment of eco-environmental quality in cities [19,20], mining areas [21,22], natural ecological areas [23,24], etc. Many studies have taken into account the regional characteristics of the study area and have made corresponding improvements to RSEI. The common method is replacing or increasing some factors in RSEI. For example, the Enhanced Vegetation Index (EVI) was used instead of normalized difference vegetation index (NDVI) [25]; the desertification index replaces the heat indicator [26]; for the Modified Remote Sensing Ecology Index (MRSEI), the soil erosion factor has been added to the RSEI [27]; the remote sensing ecological index of semi-arid region (SA-RSEI) includes the salinity and sand index [28]; for the improved remote sensing ecological index (IRSEI), the human activity intensity index has been increased to the RSEI [29]. Through the changes in the above factors, the eco-environmental quality assessment model could better adapt to the characteristics of the study area.

With the in-depth study of eco-environmental quality, the research on the relationship between urbanization and eco-environmental quality is one of the hotspots. Additionally, many related theories and methods have been produced: the environmental Kuznets curve (EKC) [30,31], Coupling Rubik's Cube [32], the coupling coordination degree (CCD) model [33,34], the urbanization and eco-environment coupling coil theory [35], etc. Among them, the CCD model is widely used to explore the coupling relationship among different systems [36–38]. For example, Li assessed the coordinated development level of the economy, society, and environment subsystem in a city [36]; Xie et al. analyzed the coordinated development of the "resources-environment-ecology-economy-society" complex system in China [37]; and Shen et al. assessed the CCD between carbon emissions and eco-environmental quality [38]. The CCD model focuses on the description of the interaction between two or more subsystems [39] and is suitable for representing the relationship between urbanization and the ecosystem [36–38]. Therefore, many studies on the relationship between urbanization and the eco-environment based on statistical data, for example, He et al. [40] examine the relationship between urbanization and the eco-environment in Shanghai; and Liu et al. [41] analyze the temporal and spatial characteristics of the coordination of urbanization and eco-environment of 30 provinces in China.

While there are a lot of relevant studies used in eco-environmental quality and urbanization, there are some limitations. a) As one of the most ecologically fragile regions in China, the Yellow River Basin is faced with the threat of worsening soil and water loss, desertification and vegetation degradation, etc. [42]. The traditional eco-environmental quality evaluation methods in this region need to integrate some factors, such as soil and water conservation, vegetation cover, hydrothermal conditions, and other aspects. However, RSEI only represents four aspects of the eco-environment: greenness, humidity, dryness, and heat. It is not applicable to the Yellow River basin with serious problems such as soil erosion and desertification. (b) Various data sources lead to greater uncertainty in quantitative analysis of relationships between urbanization and eco-environmental quality. For example, low spatial resolution data cannot support more details expressions on the pixel level, and the current research focuses on a certain scale, such as nation [43], province [33], or city [39], etc. To sum up, multi-scale quantitative analysis is lacking.

The objectives of this paper are as follows: (1) to establish an eco-environmental quality assessment model suitable for YRBU; (2) to explore the spatio-temporal variation characteristics and distribution pattern of the CCD at multi-scale perspectives: urban agglomeration, municipal, county, and pixel. That is, the paper aims to provide support for the ecological civilization construction and new-type urbanization development of YRBU. The chapters of this paper are arranged as follows: The data and methods are described in Sections 2 and 3, respectively. Section 4 presents the characteristics of the Adjusted Remote Sensing Ecological Index (A-RSEI), and multi-scale analysis of typical urban agglomerations in the upper, middle, and lower reaches; Section 5 compares A-RSEI with other methods and discusses the policy implications of the research.

2. Study Area and Data

2.1. Study Area

According to the "Planning Outline for Ecological Protection and High-quality Development in the Yellow River Basin" [44], it is proposed to divide the Yellow River Basin into five major urban agglomerations, as shown in Figure 1.

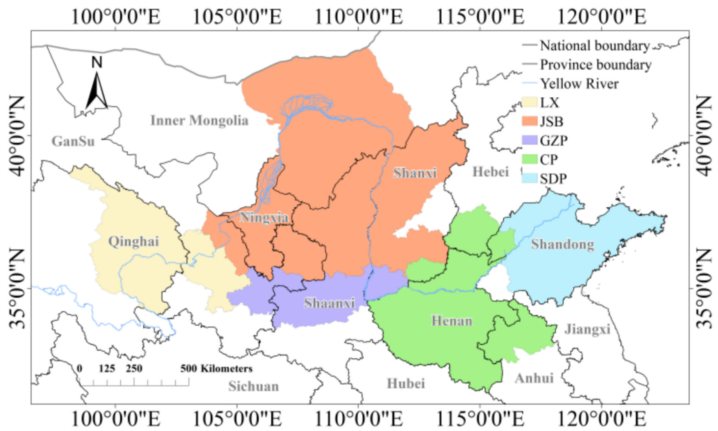

Figure 1. Spatial location map of the study area. (1) Lanxi Urban Agglomeration (LX), represents an important industrial base; (2) Ji-Shaped Bend Urban Agglomeration (JSB) represents important energy and raw material bases; (3) Guanzhong Plain Urban Agglomeration (GZP) and (4) Central Plain Urban Agglomeration (CP), represent green development demonstration zones; and (5) Shangdong Peninsula Urban Agglomeration (SDP) represents the Blue Economy Demonstration Zone.

2.2. Data

As shown in Table 1, the proposed model (A-RSEI) uses the following data to build indicators; among them, the remote sensing revised Morgan, Morgan and Finney model (RMMF) is calculated based on Sentinel-2A and Landsat8 image data, as well as MODIS LAI, digital elevation model (DEM), Soil texture data (Soil) and China Land Cover Dataset (CLCD); additionally, the normalized difference vegetation index (NDVI), land-surface temperature (LST), normalized difference build-up and soil index (NDBSI), and potential surface abundance index (SPWI) are calculated based on Sentinel-2A and Landsat8 image data. In addition, the national population density data (POP), Gross Domestic Product (GDP), and nighttime light data (VIIRS) are used to indicate the level of urbanization development.

By using Javascript programming on the Google Earth Engine (GEE) platform, Sentinel-2 and Landsat8 images were processed by cloud filtering, and various indexes such as NDVI, LST, NDBSI, SPWI and RMMF of A-RSEI were calculated, and pre-processing such as Mosaic, crop and resampling was carried out. In order to avoid the influence of water area on the humidity indicator, the Modified Normalized Difference Water Index (MNDWI) is used to remove water body information. The night light data (VIIRS) need to be corrected for saturation and continuity. The A-RSEI and the urbanization index are processed to the same spatial resolution of 100 × 100 m by the resampling method, which is used to calculate the CCD.

Table 1. Data source and description.

Data Name	Spatial Resolution	Time	Source
Sentinel-2A	10 m	2019–2021	ESA [a]
Landsat8	30 m	2013–2017	USGS [b]
MODIS LAI	500 m	2013–2021	NASA [c]
DEM	30 m	2000	NASA [c]
Soil	1 km	-	CAS [d]
CLCD	30 m	2013–2020	Paper [45]
POP	1 km	2013–2021	WorldPop [e]
GDP	1 km	2015–2019	CAS [d]
VIIRS	500 m	2014–2021	NOAA [f]
The administrative division data	1:1 million	2019	NCSFGI [g]

[a] ESA: European Space Agency. (https://www.esa.int/Science, accessed on 25 November 2022); [b] USGS: United States Geological Survey. (https://www.usgs.gov, accessed on 25 November 2022); [c] NASA: National Aeronautics and Space Administration. (https://www.nasa.gov, accessed on 25 November 2022); [d] CAS: Chinese Academy of Sciences. (http://www.resdc.cn/, accessed on 20 November 2022); [e] WorldPop: (https://www.worldpop.org, accessed on 20 November 2022); [f] NOAA: National Oceanic Atmospheric Administration. (https://www.noaa.gov, accessed on 20 November 2022); [g] NCSFGI: National Catalogue Service for Geographic Information. (https://www.webmap.cn/, accessed on 20 November 2022).

3. Methods

3.1. A-RSEI

Combined with the characteristics of the study area, especially water and soil loss, RMMF [46], as the model for water and soil conservation, is introduced into the A-RSEI model based on RSEI. Additionally, SPWI [47] is used to replace the original humidity indicator. This can effectively reflect the spatial distribution of surface water resources, indicate the richness of surface water resources, and truly express the impact of water resources on the ecological environment. Therefore, the entropy weight method is used to construct A-RSEI by combining five sub-indicators of greenness, heat, dryness, humidity, and water and soil conservation. Additionally, NDVI, LST, NDBSI, SPWI, and RMMF are calculated by the GEE platform, which are used to represent greenness, heat, dryness, humidity, and water and soil conservation, respectively.

NDVI has been widely used to monitor vegetation properties, such as fractional vegetation coverage, plant biomass and leaf area. It can reflect the effective indicator of vegetation growth, and is also one of the important ecological indicators [48].

$$NDVI = (\rho_{nir} - \rho_{red})/(\rho_{nir} + \rho_{red}) \tag{1}$$

where ρ_{nir}, ρ_{red} denote the reflectance of the near-infrared and red bands in Sentinel-2A and Landsat8.

LST is an important indicator affecting vegetation growth and environmental change [49]. The formula is as follows:

$$L_s = B(T_s) = \frac{[L_\lambda - L_\uparrow - \tau(1-\varepsilon)L_\downarrow]}{\tau\varepsilon} \tag{2}$$

$$T_s = \frac{K_2}{\lambda \ln\left(1 + \frac{K_1\lambda^{-5}}{L_s}\right)} \tag{3}$$

where: ε is the surface emissivity; T_s is the real surface temperature (K); $B(T_s)$ is the brightness of blackbody thermal radiation; τ is the transmittance of atmosphere in thermal infrared band; and $L_\uparrow$ and $L_\downarrow$ are the brightness of upward and downward atmospheric radiation, respectively.

The calculation formula of SPWI is as follows [47]:

$$SPWI = \frac{\rho_{nir} - \rho_{swir2} + \rho_{blue}}{\rho_{nir} + \rho_{swir2} + \rho_{blue}} \tag{4}$$

where ρ_i is the reflectance of Sentinel-2A and Landsat8 corresponding to band i.

NDBSI reflect the damage to natural landscapes caused by the rapid expansion of building land and bare soil exposure. The related formula is as follows [50,51]:

$$NDBSI = (IBI + SI)/2 \tag{5}$$

$$SI = \frac{(\rho_{swir1} + \rho_{red}) - (\rho_{nir} + \rho_{blue})}{(\rho_{swir1} + \rho_{red}) + (\rho_{nir} + \rho_{blue})} \tag{6}$$

$$IBI = \frac{2\rho_{swir1}/(\rho_{swir1} + \rho_{nir}) - [\rho_{nir}/(\rho_{nir} + \rho_{red}) + \rho_{green}/(\rho_{green} + \rho_{swir1})]}{2\rho_{swir1}/(\rho_{swir1} + \rho_{nir}) + [\rho_{nir}/(\rho_{nir} + \rho_{red}) + \rho_{green}/(\rho_{green} + \rho_{swir1})]} \tag{7}$$

RMMF evaluated the soil and water conservation function of the ecosystem based on three aspects: regional unit precipitation interception rate, regional unit runoff erosion amount, and regional unit runoff transportation amount [52]. It can objectively reflect the water and soil conservation function of ecosystem based on remote sensing data [46].

In order to eliminate the influence of different indicator dimensions on the results, dimensionless processing is needed for all indicators. The range standard method was used to standardize the five indicators in A-RSEI. The indicators are divided into positive indicators and negative indicators. The positive indicators include NDVI, SPWI and RMMF, while the negative indicators include LST and NDBSI. The standardized equation is as follows [43]:

$$r_s^+ = (I_j - I_{min})/(I_{max} - I_{min}) \tag{8}$$

$$r_s^- = (I_{max} - I_j)/(I_{max} - I_{min}) \tag{9}$$

where r_s^+ and r_s^- represent the standardized values of the jth positive indicator and the negative indicator, respectively; I_j is the original value of the jth indicator; I_{min} and I_{max} are the minimum and maximum values of the jth indicator.

Through ArcGIS software, the entropy weight method is used to integrate the above indicators for calculating the evaluation results of eco-environmental quality and urbanization. It is mainly to assign appropriate weight to each indicator by evaluating the degree of difference between indicators.

First, the weight of each indicator is calculated.

$$e_j = \frac{1}{\ln n} \times \sum_{i=1}^{n} f_{ij} \ln f_{ij} \tag{10}$$

$$f_{ij} = \frac{x_{ij}}{\sum_{i=1}^{n} x_{ij}} \tag{11}$$

where: e_j is the entropy value of the jth evaluation indicator; and f_{ij} is the weight corresponding to the jth indicator of the ith pixel.

Secondly, set w_j as the entropy weight of the jth evaluation indicator. The entropy weight w_j is calculated as follows:

$$w_j = \frac{1 - e_j}{m - \sum_{i=1}^{m} e_i}, \quad j = 1, 2, 3, \ldots, m \tag{12}$$

where: e_j is the entropy of the jth indicator; m is the number of indicators; and w_j is the weight corresponding to the w_j indicator.

Finally, the linear weighting method is used to fuse each indicator to ensure the overall homogeneity of the results.

3.2. Urbanization Indicator

Urbanization is characterized by population growth, economic development and urban spatial density. Thus, the quantification of urbanization can be realized from three aspects [53]: population density, GDP density and night light intensity. Because the spatial distribution of the three aspects is highly similar, the three indicators can be integrated into a comprehensive indicator after being standardized by entropy weight method. The comprehensive indicator is called the comprehensive level of urbanization (CUL). The formula is as follows:

$$CUL_i = \sum_{k=1}^{3} W_k \times X_{(i,k)} \tag{13}$$

where CUL_i is the urbanization index in the i year; W_k represents the weight of the indicator; and $X_{(i,k)}$ represents the standardized value of the indicator in the year.

3.3. CCD

Based on ArcGIS software, this study explored the coupling mechanism between the eco-environmental quality and urbanization in the YRBU using the CCD model. The formula of CCD model is as follows [43,54]:

$$C = \left\{ \frac{U \times E}{[(U+E)/2]^2} \right\}^{\frac{1}{2}} \tag{14}$$

$$CCD = \sqrt{C \times T} \tag{15}$$

$$T = \alpha U + \beta E \tag{16}$$

where C was the coupling degree; U was the urbanization index; E was the eco-environmental quality index; and CCD is the coupling coordination degree, and its value ranges from 0 to 1, where the higher CCD indicated the higher the level of coordinated development between eco-environmental quality and urbanization (Table 2). T was the comprehensive evaluation index of U and E, and α and β were the weights of U and E, respectively, where $\alpha + \beta = 1$. Because the eco-environmental quality and urbanization had the same interaction, α and β were set as 0.5 in this study, respectively [54].

Table 2. Coupling coordination level assessment.

Range of CCD	Coordination Level	Range of CCD	Coordination Level
0.0000–0.1	Extremely out of coordination	0.5001–0.6	Marginal coordination
0.1001–0.2	Seriously out of coordination	0.6001–0.7	Primary coordination
0.2001–0.3	Medium dysfunction	0.7001–0.8	Moderate coordination
0.3001–0.4	Mild dysfunction	0.8001–0.9	Good coordination
0.4001–0.5	Close to dysfunction	0.9001–1.0	High-quality coordination

3.4. Spatial Autocorrelation

Based on GeoDa software, Moran method is used to represent global spatial autocorrelation of the study area. Additionally, the local spatial autocorrelation is quantified by LISA.

$$global\ Moran's\ I = \frac{n \sum_{i=1}^{n} \sum_{j=1}^{n} W_{i,j} (x_i - \overline{x}) (x_j - \overline{x})}{\left(\sum_{i=1}^{n} \sum_{j=1}^{n} W_{i,j} \right) \sum_{i=1}^{n} (x_i - \overline{x})^2} \tag{17}$$

$$LISA = \frac{x_i - \overline{x}}{\sum_{j=1, j \neq i}^{n} (x_j - \overline{x})^2} \sum_{j=1, j \neq i}^{n} W_{i,j} (x_j - \overline{x}) \tag{18}$$

where: x_i and x_j represent the variable values at i and j; $\overline{x}$ is the average value; n is the number of sample pairs; $W_{i,j}$ is the spatial weight function; the $global\ Moran's\ I$ value range is $(-1, 1)$, and the closer it is to 1, the higher the clustering degree will be. The results of local spatial autocorrelation analysis produced a LISA cluster map, which presented five spatial distribution types: high–high cluster (HH), low–low cluster (LL), high–low outliers (HL), low–high outliers (LH), and insignificant.

3.5. The Tapio Decoupling Model

Tapio Decoupling Model is established according to the ratio of the change rate of eco-environmental quality level (ΔE) to the change rate of urbanization level (ΔU). It reflects the dynamic relationship between eco-environmental quality and urbanization [55]. The Tapio decoupling model subdivides decoupling into eight categories (Table 3): declining decoupling, strong decoupling, weak decoupling, expansion connection, recessive connection, expansion negative decoupling, strong negative decoupling, and weak negative decoupling [56,57].

$$DI_t = [-(E_t - E_{t-1})/E_{t-1}]/[(U_t - U_{t-1})/U_{t-1}] \tag{19}$$

where DI_t is the decoupling index; E_t and E_{t-1} are the eco-environmental quality in years t and $t-1$; U_t and U_{t-1} are the urbanization in years t and t-1.

Table 3. Evaluation of decoupling level between urbanization and eco-environmental quality.

Decoupling Status		ΔE	ΔU	DI
Decoupling	Strong decoupling	-	+	DI < 0
	Weak decoupling	+	+	$0 \leq$ DI < 1.2
Negative Decoupling	Expansion negative decoupling	+	+	DI $\geq$ 1.2
	Strong negative decoupling	+	-	DI < 0
	Weak negative decoupling	-	-	$0 \leq$ DI < 0.8
Recessive decoupling	Recessive decoupling	-	-	DI $\geq$ 1.2
Connection	Expansion connection	+	+	$0.8 \leq$ DI $\leq$ 1.2
	Recessive connection	-	-	$0.8 \leq$ DI $\leq$ 1.2

4. Results

4.1. Applicability Evaluation of A-RSEI

In order to verify the applicability of A-RSEI to the study area, firstly, collinear diagnostic indicators in linear regression were used to explore the redundancy of the selected indicators and verify the rationality of the selection of indicators. The variance inflation factor (VIF) and tolerance (TOL) are reciprocal of each other, which are common indicators of collinearity diagnosis. When VIF<10 or TOL>0.1, indicated that the selected evaluation indicator is reasonable. In this study, pixel values of all indicators are extracted, and the redundancy is analyzed. The diagnostic results are shown in Table 4. The results show that five indicators are reasonable, and there is no information redundancy among the indicators.

Table 4. Collinearity diagnosis results.

Indicator	VIF	TOL
LST	1.400	0.714
NDBSI	4.503	0.222
NDVI	3.374	0.296
RMMF	3.800	0.263
SPWI	2.302	0.434

Then, we evaluated the A-RSEI and RSEI's regional adaptability compared to the Ecological Index (EI). Figure 2a shows that the RSEI index was significantly overestimated from the deviation between the fitting line and the 1:1 line. Additionally, the proposed A-RSEI model has improved the overestimation phenomenon, as shown in Figure 2b, the RMSE decreased from 0.174 to 0.082, and R2 increased from 0.9742 to 0.9883. Overall, the accuracy of the A-RSEI model is better than that of the RSEI model in the study area.

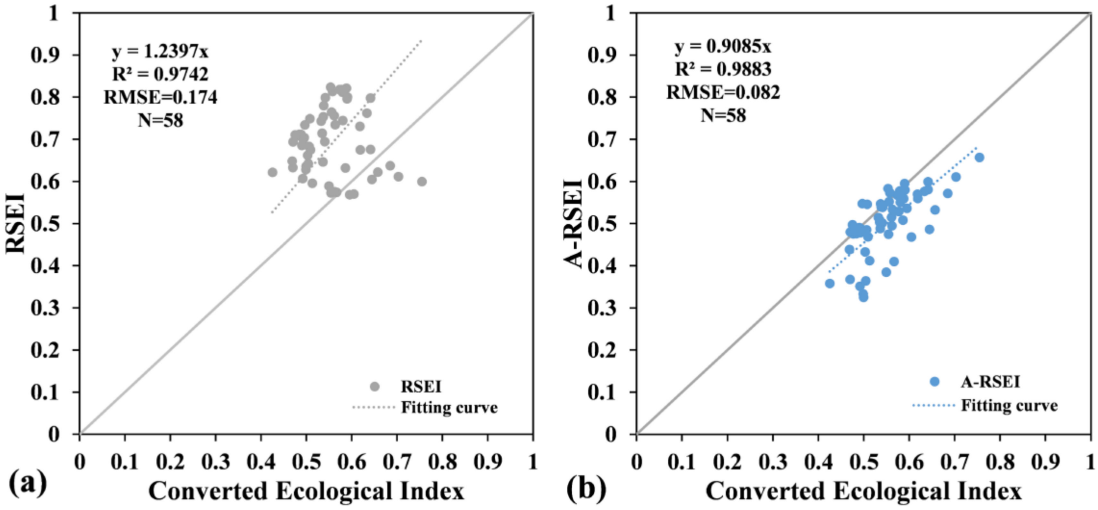

Figure 2. The regional adaptation assessment results for RSEI (**a**) and A-RSEI (**b**) using EI. Discrete points in gray are the corresponding EI and RSEI values of each cities in the study area, while discrete points in blue are the corresponding EI and A-RSEI values of each cities in the study area.

4.2. Multi-Scale Analysis of A-RSEI, Urbanization and CCD

4.2.1. Urban Agglomeration Perspective

The growth rates of eco-environmental quality, urbanization and CCD in the whole study area are 0.007418, 0.004260 and 0.009006, respectively. The highest and lowest trend values were 0.009953 and 0.002484, respectively, for GZP and LX. The urbanization and CCD of the CP urban agglomeration have the largest upward trend, with the change rates of 0.009537 and 0.013985 (Table 5). As show in Figure 3, the A-RSEI, urbanization and CCD of the five sub-urban agglomerations has showed a positive rate from 2013 to 2021, while the value of A-RSEI decreased in 2019. The urbanization and CCD have expressed the same rank order as follows: SDP > CP > GZP > JSB > LX. Compared with 2013, the urbanization and CCD of the study area in 2021 increased by 35.19% and 14.64%, respectively (Figure 3b,c).

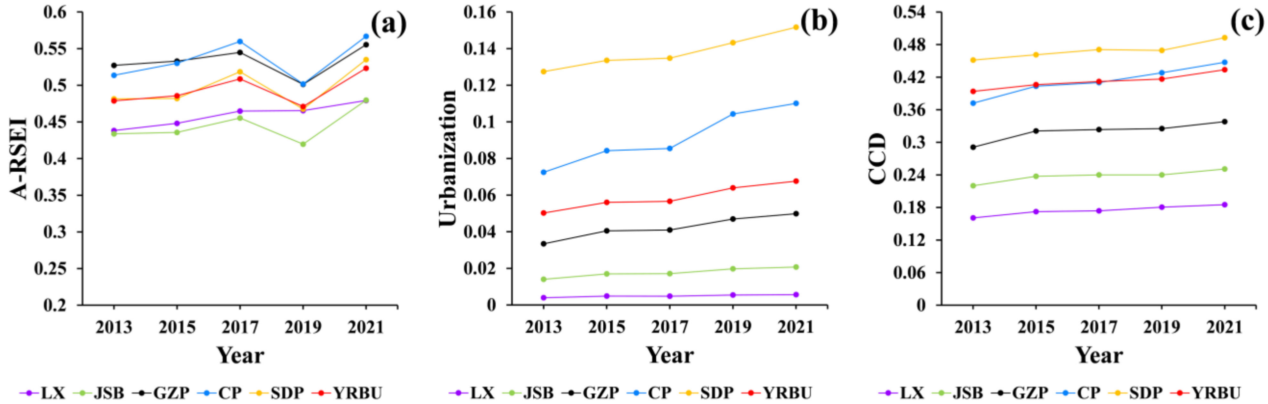

Figure 3. The dynamic change in the mean A-RSEI (**a**), Urbanization (**b**) and CCD (**c**) in the Yellow River Basin Urban Agglomeration (YRBU) and its sub-urban agglomeration (LX, JSB, GZP, CP, SDP), from 2013 to 2021.

Table 5. The change rates (a^{-1}) of the A-RSEI, Urbanization, and CCD for sub-urban agglomeration and the entire study area.

Region	A-RSEI	Urbanization	CCD
LX	0.009953	0.000401	0.005699
JSB	0.007587	0.001612	0.008121
GZP	0.002484	0.003938	0.009576
CP	0.007831	0.009537	0.013985
SDP	0.009233	0.005813	0.007695
Study area	0.007418	0.004260	0.009006

4.2.2. Municipal-Scale Perspective

From the municipal-scale perspective, the spatial distribution of A-RSEI, urbanization and CCD showed the characteristics of "high in the east, low in the west" (Figure 4). Specifically, A-RSEI showed a decreasing trend from southeast to northwest, indicating that the cities with higher eco-environmental quality were mainly distributed in the GZP and the southeastern part of the CP. For example, Baoji City in Shaanxi Province was always at a high level of eco-environmental quality. Compared with 2013, the overall eco-environmental quality of all cities will be improved in 2021. The change rate of cities with a higher growth rate presents a distribution of "faster in the east and west, slower in the middle " (Figure 5a). Only two cities in the west of GZP, namely, Tianshui City in Gansu Province and Baoji City in Shaanxi Province, have showed negative change rates.

The rapid growth of urbanization and the CCD are mainly distributed in the southeast of CP. For example, the urbanization mainly takes Zhengzhou City–Qingdao City as the poles, showing a trend of outward-radiating development. Only Haibei Tibetan Autonomous Prefecture of Qinghai Province shows a negative trend, with a change value of -0.001366 (Figure 5b). From 2013 to 2021, the number of coordinated cities has increased from 9 to 33, while the number of uncoordinated cities has decreased from 65 to 43 (Figure 6a).

4.2.3. County-Scale Perspective

Compared with the municipal-scale perspective, it can be clearly seen from the county-scale perspective that the eco-environmental quality of the counties with higher urbanization level in the southeast is usually lower than that of the surrounding counties, especially the urban area of Xi 'an in Shaanxi Province. The surrounding counties of Xi 'an, such as Fengxian County, Taibai County and Zhouzhi County, have always maintained a higher eco-environmental quality. However, it can also be found that while the eco-environmental quality and urbanization level of the urban area centered on Xi 'an, the eco-environmental quality of the surrounding counties has declined to a certain extent (Figure 7).

From 2013 to 2021, the proportion of counties with the highest eco-environmental quality in the study area increased from 1.2% in 2013 to 3.6% in 2021. Overall, 90.57% of the counties had a positive change rate. Then, the proportion of counties with coordination in the study area increased from 24.06%, in 2013, to 45.86%, in 2021 (Figure 6b). It means that the coupling coordination degree between eco-environmental quality and urbanization level at the county level has been improved. In particular, the highest trend values were 0.0401 for Huanglong County (Figure 5c).

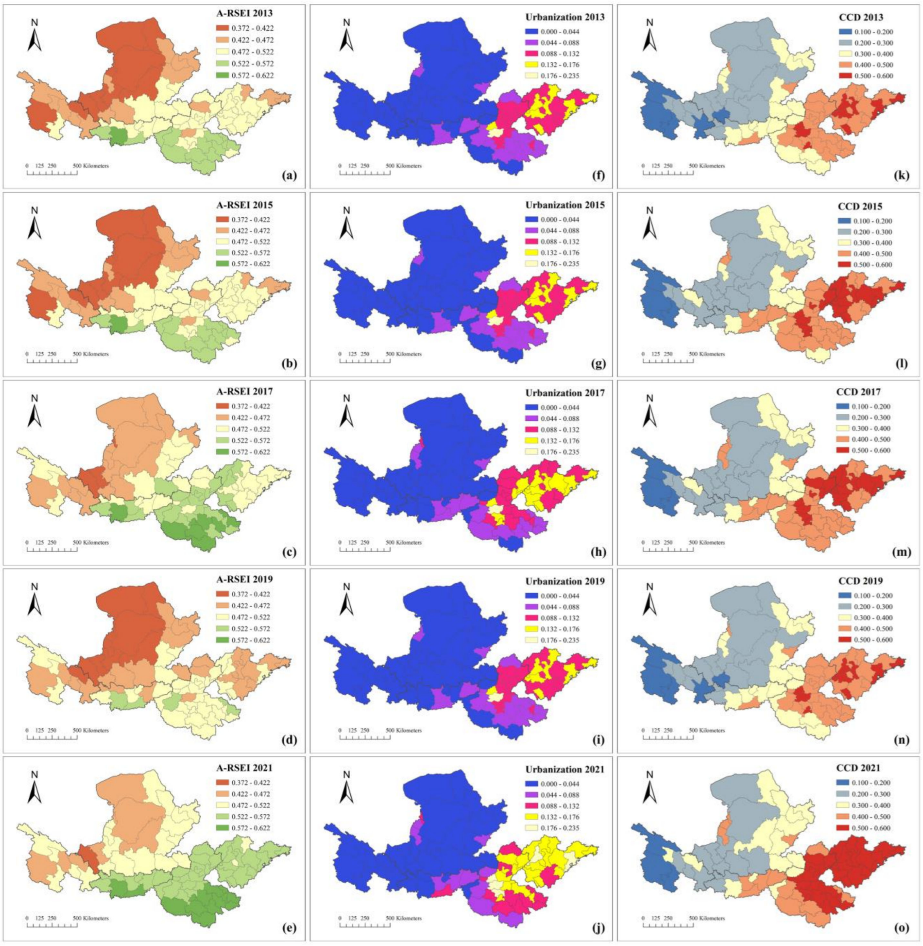

Figure 4. Spatial distribution in the Yellow River Basin Urban Agglomeration (YRBU) of the A-RSEI (**a**–**e**), Urbanization (**f**–**j**) and CCD (**k**–**o**) from 2013 to 2021 at municipal-scale perspective.

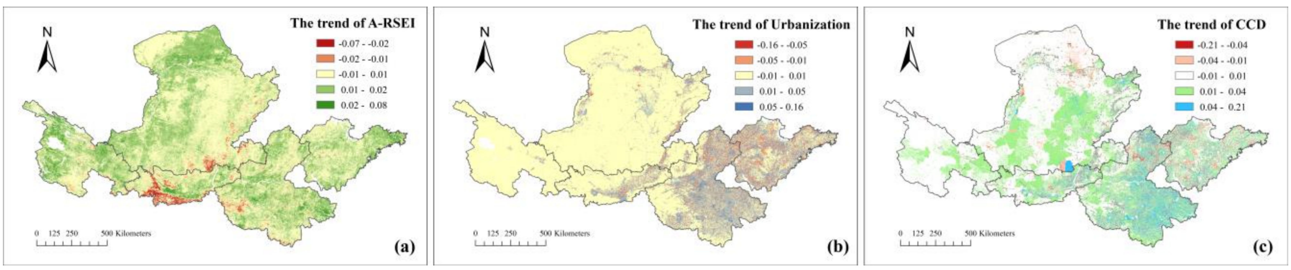

Figure 5. Spatial distributions in the Yellow River Basin Urban Agglomeration (YRBU) of the A-RSEI's change rates (**a**), urbanization's change rates (**b**) and CCD's change rates (**c**) in the study area, during 2013–2021, at pixel-scale perspective.

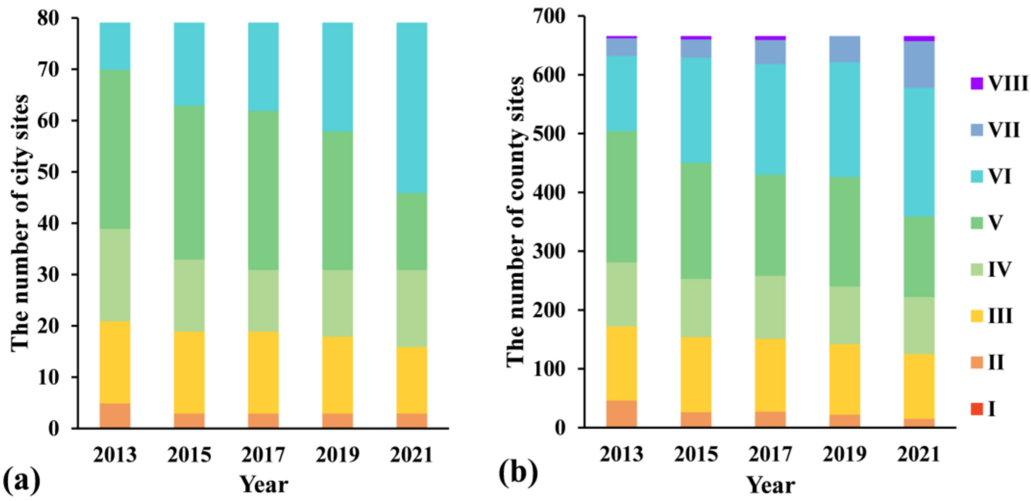

Figure 6. The statistical graph of the number of cities (**a**) and counties (**b**) with different CCD levels. (I) Extremely out of coordination. (II) Seriously out of coordination. (III) Medium dysfunction. (IV) Mild dysfunction. (V) Close to dysfunction. (VI) Marginal coordination. (VII) Primary coordination. (VIII) Moderate coordination.

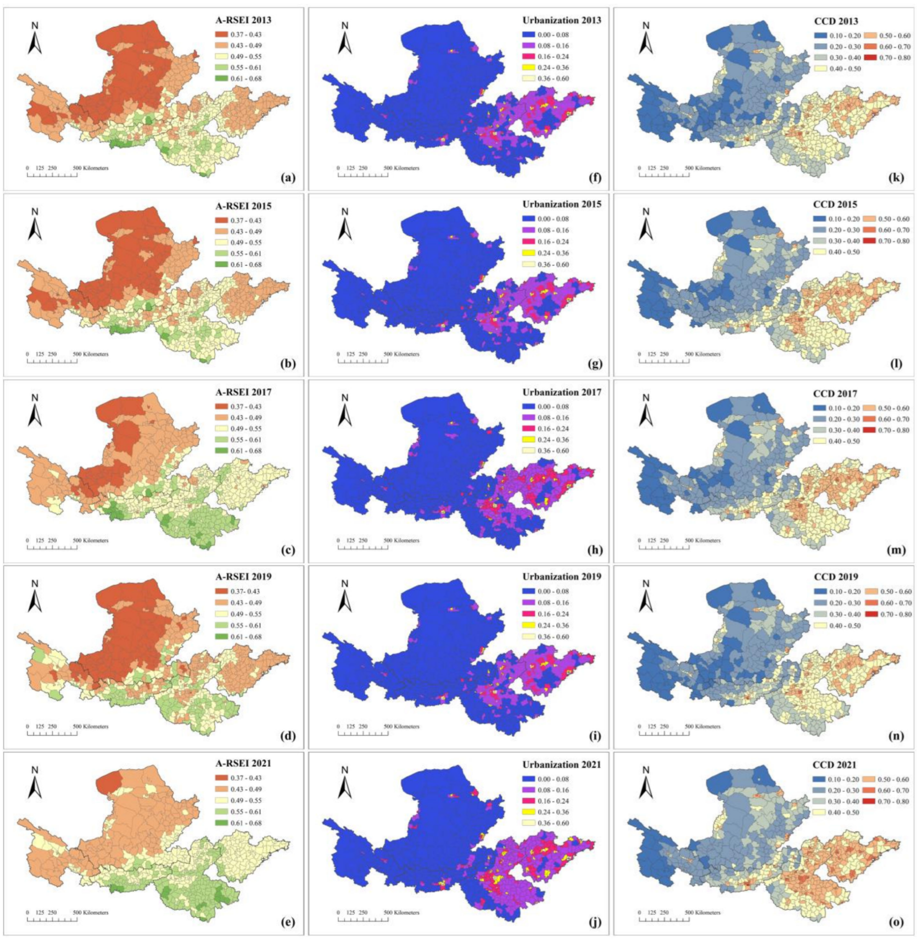

Figure 7. Spatial distribution in the Yellow River Basin Urban Agglomeration (YRBU) of the A-RSEI (**a**–**e**), Urbanization (**f**–**j**) and CCD (**k**–**o**), from 2013 to 2021, at county-scale perspective.

4.2.4. Pixel-Scale Perspective

From the pixel-scale (Figure 8), it can be seen that Hetao Plain, Longzhong Loess Plateau and other regions present lower eco-environmental quality. However, at the same time, the eco-environmental quality of this region has been continuously improved (Figures 5 and 8). Moreover, its urbanization distribution shows an obvious trend of radiating outward from the area, which has the characteristics of high urbanization in the central region. These are distributed along the Yellow River in areas with low elevation and flat terrain, such as Guanzhong Basin, Fenhe Valley, Taiyuan Basin and Huang-Huai-Hai Plain.

In addition, the eco-environmental quality of the regions with a higher degree of urbanization will be worse than that of the surrounding areas. For example, Qinling Mountains and Taiyue Mountains presents a negative change rate. Additionally, the areas in Guanzhong Basin show a lower eco-environmental quality compared with the surrounding areas (Figure 8).

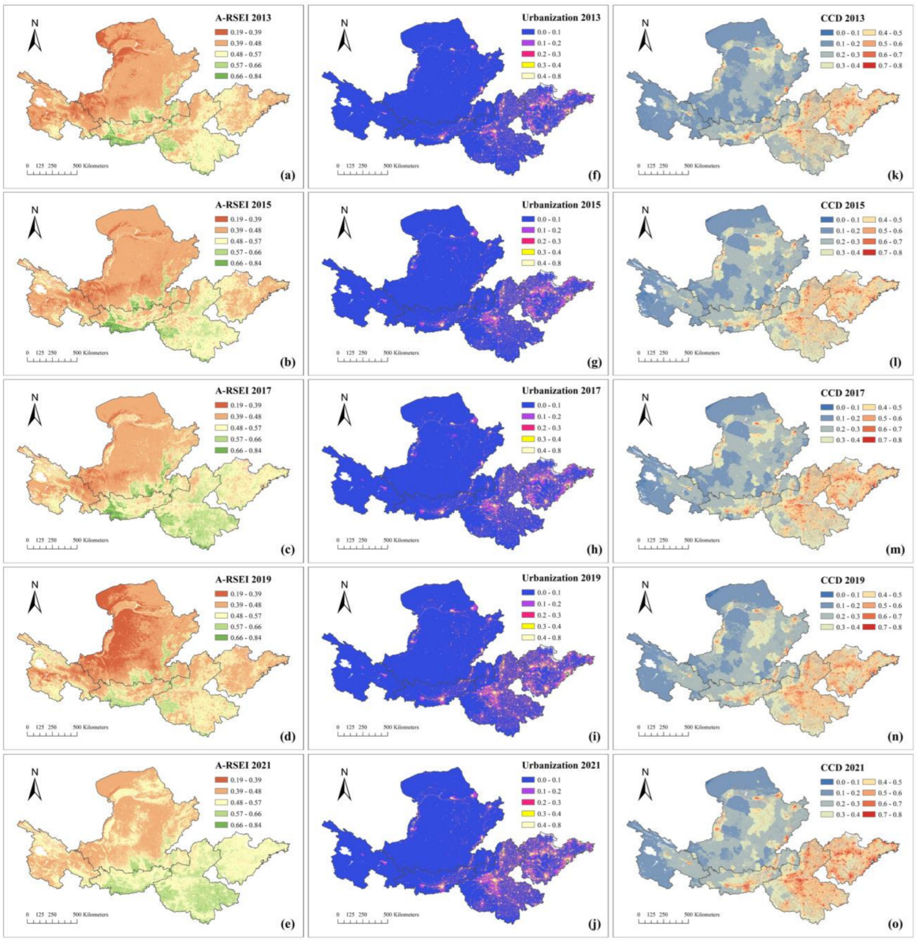

Figure 8. Spatial distribution in the Yellow River Basin Urban Agglomeration (YRBU) of the A-RSEI (**a**–**e**), Urbanization (**f**–**j**) and CCD (**k**–**o**), from 2013 to 2021, at pixel-scale perspective.

4.3. Spatio-Temporal Characteristics of CCD

4.3.1. Spatial Autocorrelation Analysis of CCD

As shown in Figure 9, from 2013 to 2021, the global Moran's I value of CCD is positive, and the Moran's I value at the municipal-scale is always larger than that at the county-scale. Additionally, the global Moran's I value at the municipal-scale and county-scale showed an overall upward trend. This means that the concentration degree of coupling relationship has increased significantly from 2013 to 2021.

The spatial distribution of CCD values at both county-scale and municipal-scale perspective showed obvious agglomeration characteristics. From the municipal-scale perspective, the HH type regions are mainly distributed around the provincial capitals of SDP and CP. The scope of HH type region centered on Zhengzhou has a trend of gradual expansion, and gradually expands to the southeast region. The size of HH type area with Ji 'nan as the center showed a trend of "increasing-decreasing" fluctuation (Figure 9a–c).

From the county-scale perspective, it can be seen that there are small areas of GZP that show HH type, and they are mainly distributed in Xi 'an, the provincial capital city of Shaanxi Province. However, the LL type areas are widely distributed in the northwestern LX and JSB. From the county-scale perspective, the size of the LL type area has no significant change, while the size of LL type area is gradually expanding from the municipal-scale perspective (Figure 9d–f).

In addition, compared with the municipal-scale, the study area also shows LH type and HL type regional distribution at the county-scale. The LH type is mainly distributed around the HH city cluster in the CP. Additionally, the LH type area in the CP gradually disappeared from 2013 to 2021, and part of it changed into HH type. Therefore, the HH type area in the center of CP has a driving effect on LH type area.

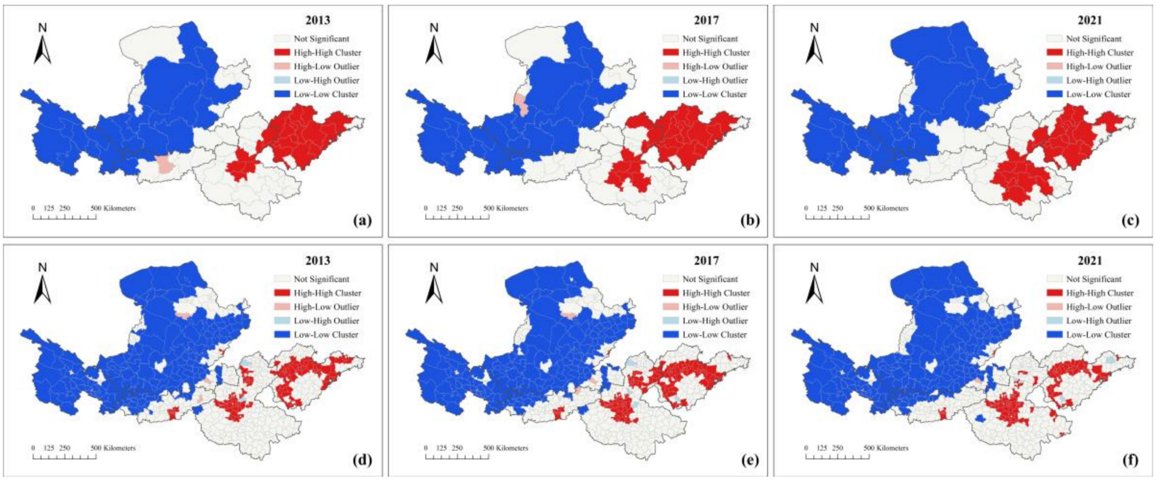

Figure 9. The local autocorrelation cluster maps in the Yellow River Basin Urban Agglomeration (YRBU) at the municipal-scale (**a**–**c**) and county-scale (**d**–**f**), during 2013, 2017, and 2021.

4.3.2. Decoupling Analysis of CCD

As can be seen from Figure 10e, strong decoupling and weak decoupling are mainly distributed from 2013 to 2021 in the study area. Compared with 2013, 96.20% of the cities showed strong decoupling in 2021. The strong decoupling state shows that the ecological environment in the study area has been improved in the process of urbanization development, and the urban development has the characteristics of green and low carbon.

From 2013 to 2015, 60.76% of cities were in the state of strong decoupling, and 30.38% were in the state of weak decoupling. Weak decoupling was mainly distributed in the eastern part of the JSB. However, in this region, the growth rate of urbanization level is higher than that of the reduction in eco-environmental quality, which is expected to develop towards a strong decoupling pattern (Figure 10a). From 2015 to 2017, 86.08% of the city's CCDs are in a strong decoupling state, and some cities are in a recession decoupling state, which are mainly distributed in the western region of the study area (Figure 10b). From 2017 to 2019, weak decoupling dominated most of the study areas, accounting for 67.09%. However, there were some areas with extended negative decoupling and strong negative decoupling, which were distributed in the SDP and the northern JSB. This indicates that the study area at this stage is in a relatively good decoupling pattern, but some areas need to pay attention to eco-environmental quality (Figure 10c). From 2019 to 2021, the study area only showed strong decoupling and weak decoupling, indicating that most cities in the study area were in an ideal decoupling state (Figure 10d).

In general, it can be seen that most of the study areas are in a strong decoupling and weak decoupling state. It shows that the coupling and coordination relationship between the ecological environment and urbanization in the study area has continued to rise.

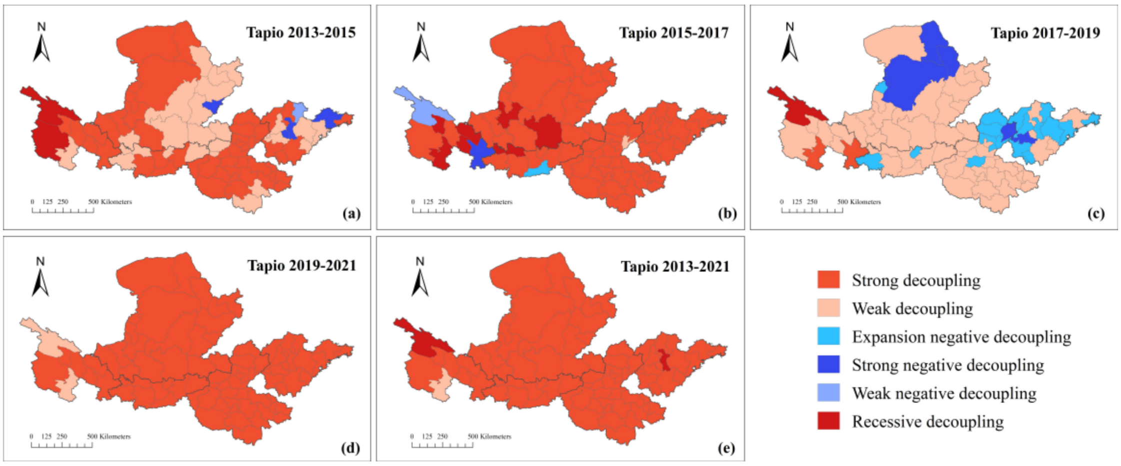

Figure 10. Decoupling distribution map in the Yellow River Basin Urban Agglomeration (YRBU), 2013–2015 (**a**), 2015–2017 (**b**), 2017–2019 (**c**), 2019–2021 (**d**), and 2013–2021 (**e**).

4.4. Multi-Scale Analysis in the Upper, Middle and Lower Reaches

The performance of ecological environment resources, total population and economic development express spatial imbalance in the upper, middle and lower reaches of the Yellow River Basin. The overall trend of CCD change has the characteristics of "faster in the east and slower in the west", which is similar to the characteristics observed in the trend of urbanization. For multi-scale quantitative analysis, LX, JSB and CP are used as the typical areas in the upper, middle and lower reaches, respectively. From 2013 to 2021, CCD in all the cities of the three urban agglomerations showed an upward trend. As can be seen from Figure 11, The CCD growth in the CP is significantly faster than that in LX.

- Lanxi Urban agglomeration (LX) in the upper reaches

At the urban agglomeration scale, urbanization development has a positive impact on the ecological environment. The overall distribution is more obvious on the pixel-scale. From Figure 8, it can be seen that the regions with higher development rates of CCD relationships are located in the eastern low altitude regions, which may be due to the effect of factors such as the topography, water resources and transportation conditions. From the municipal-scale perspective, the CCD in Lanzhou is more prominent than other cities (Figure 4). It can be found that the areas with higher coupling coordination in the region are mainly distributed in its main urban area, and the CCD in the southeastern part of the city shows a wide range of slight improvement trends (Figure 11b). Taking Yuzhong County as an example, most areas show slight improvement of CCD at the county-scale (Figure 11c).

- Ji-Shaped Bend Metropolitan Area (JSB) in the middle reaches

The eco-environmental quality is high in the east and low in the west (Figure 4), with the western regions with the higher eco-environmental quality being mostly distributed in Hetao Plain and Ningxia Plain (Figure 8). The reasons for that are flat terrain, suitable environment and concentrated industrial distribution. From the municipal-scale perspective, the CCD of Yinchuan city is more prominent than that of other cities (Figure 11e). From the county-scale perspective, the CCD in Xingqing has shown significant improvement, and the eco-environmental quality and urbanization level of this area have also gradually increased (Figure 11f).

The reasons for that include the rich resources such as the National Wetland Park, and the continuous improvement of its tourism industry development level in recent years to promote the growth of the national economy.

- Central Plains urban agglomeration (CP) in the lower reaches.

The eco-environmental quality of CP is low in the northwest and high in the southeast. The urbanization presents a spatial distribution pattern with Zhengzhou as the core and radiating around (Figure 8). From 2013 to 2021, the urbanization growth rate is 1.88 (10^{-2}/a), which indicates that the urbanization development is relatively fast. From the municipal-scale perspective, the regions where the CCD degraded significantly show scattered distribution (Figure 11g). The CCD in Anyang showed obvious degradation (Figure 11h). The reasons are as follows: (a) the city is rich in mineral resources, and its urbanization development is high as a resource-based city; (b) taking steel and coal as its main industries is easy to cause certain impact on the environment.

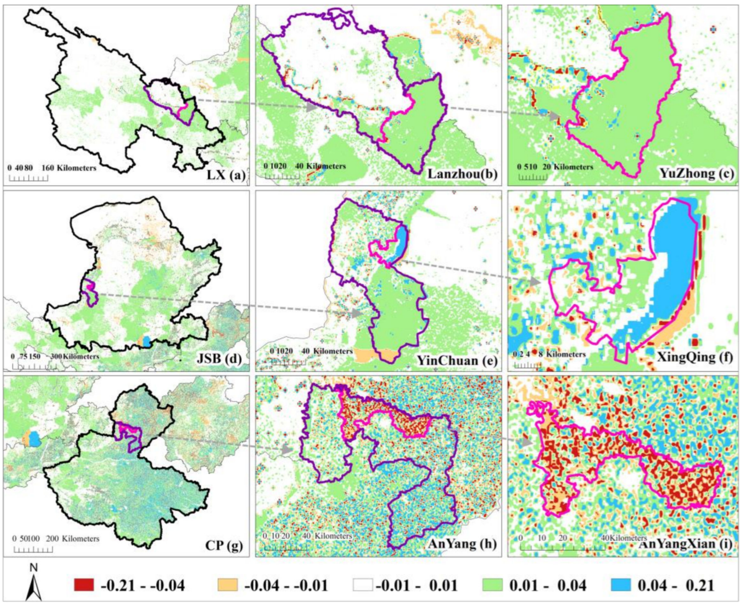

Figure 11. Spatial distribution of trends in CCD at the Lanxi (LX) urban agglomeration (**a**–**c**), Ji-Shaped Bend Metropolitan Area, and Central Plains (CP) urban agglomeration (**g**–**i**), from urban agglomeration, city level and county level. (**a**,**d**,**g**) Urban agglomeration scale; (**b**,**e**,**h**) municipal-scale; (**c**,**f**,**i**) county-scale.

5. Discussion

5.1. Characteristics of A-RSEI

The YRBU has a unique geographical location and climatic conditions. In this region, the climate is arid, semi-arid, semi-humid and humid from west to east, and the natural geographical environment varies significantly [42,58]. Additionally, there are problems such as soil erosion, desertification, and vegetation degradation. The proposed model (A-RSEI) focuses on water and soil conservation, and the five indicators reflect the characteristics of the study area from different perspectives. The greenness reflect the health and coverage of vegetation; dryness reflect the degree of bare and dry surface; the spatial pattern of surface temperature is reflected by heat; humidity reflect the moisture of soil and vegetation on the surface; and soil and water conservation reflect soil erosion and water loss in the region.

The collinearity test results show that A-RSEI selects reasonable indexes without information redundancy. Additionally, RMMF and SPWI indicators in A-RSEI play an important role. RMMF takes into account the physical mechanism of sand production and quicksand in the process of erosion and describes soil erosion more clearly [46,47]. Therefore, it is less affected by precipitation and other factors, and can objectively reflect the water and soil conservation function of the ecosystem. The humidity indicator of SPWI can effectively reflect the spatial distribution of surface water resources, thus representing the impact of water on the ecological environment in the study area.

The general trend of ecological monitoring in the Yellow River Basin by A-RSEI and RSEI is the same. That the spatial distribution of eco-environmental quality in the YRBU is mainly "high in the southeast and low in the northwest", showing obvious spatial heterogeneity. Additionally, the regions with higher eco-environmental quality are concentrated in the northern foot of the Qinling Mountains, Liupan Mountain, Ziwuling Mountain, Luliang Mountain and other national nature reserves (Figure 8). The eco-environmental quality of the whole study area showed an overall improvement, and 84.53% of the area showed an upward trend (Figure 5). The eco-environmental quality in some areas showed a downward trend, mainly concentrated in the southern part of GZP and the western part of CP (Figure 5a). This is related to the frequent human economic activities in the surrounding cities, which cause great disturbance to the eco-environment and lead to the degradation of areas with good eco-environmental quality [25] (Figure 8). This is consistent with the results of previous studies [25,58,59].

The comparisons of A-RSEI and EI and of RSEI and EI showed that the accuracy of the A-RSEI model is better than that of the RSEI model, and the RSEI index is obviously overestimated. The specific comparative analysis between the A-RSEI and RSEI also shows that the A-RSEI can better reflect the eco-environmental quality of soil and water loss areas. Although the general trend of ecological monitoring in the Yellow River Basin by the A-RSEI and RSEI is the same, there are differences in the specific spatial distribution and degree. In the area with serious soil erosion and ecological deterioration, A-RSEI has a lower value than RSEI and is closer to EI. For example, Qingyang City in Gansu Province is a typical loess plateau region where drought disasters occur frequently [60], and the A-RSEI and RSEI values of Qingyang City are 0.49 and 0.55, respectively. As for Baiyin City of Gansu Province and Shizuishan City of Ningxia, they are the mining cities that emerged with the mining of mineral resources and coal resources, as typical resource-based cities, are faced with the problems of resource exhaustion and ecological deterioration [61,62], and A-RSEI value is also more reasonable in this region.

5.2. Implcations and Further Research

From the perspective of the study area or urban agglomeration, the development trend of the whole and large region can be grasped. Then, combined with the perspective of municipal, county, and pixel scales, specific situations and specific analyses can be made. According to the temporal and spatial characteristics of ecological environment quality, urbanization, and CCD, the following three aspects are analyzed.

(1) LX and JSB should develop a comprehensive development model, because they belong to regions with low eco-environmental quality, urbanization, and CCD (Figure 3). Additionally, it is related to the regional location and economic development mode. On the one hand, there are droughts and less rain, serious soil and water loss, and other problems in this region, and the ecological environment is relatively weak [42]. On the other hand, there are many resource-based cities, which mainly carry out mining and processing of mineral resources, forests, and other resources, and it has a certain impact on eco-environmental protection [58].

With the implementation of the Yellow River Basin comprehensive planning, national new-type urbanization planning, and other policies, the eco-environmental quality and urbanization levels of the region increased by $0.00877a^{-1}$ and $0.0010065a^{-1}$, respectively (Figure 5a,b). Among them, the regions with high urbanization level and rapid urbanization growth are mainly concentrated in Lanzhou, Xining, and Yinchuan, but the significant decrease in CCD also mainly occurs in this region (Figure 11a,d), and its urbanization development has a negative impact on the ecological environment.

Therefore, regional development should pay more attention to scientific and technological innovation, promote the coal industry and energy industry to introduce high technology, and promote low-carbon development [63,64]. At the same time, it should strengthen the construction of public green spaces such as park green space, protective green space and so on [62].

(2) GZP should develop an ecological characteristic industry development mode, because the urbanization and CCD of GZP is low, but the eco-environmental quality is high (Figure 3). It has advantages in the ecological environment.

The Qinling Mountains need ecological protection. As can be seen from Figure 8e, the eco-environmental quality of Qinling Mountains has always been at a high level, but 18.67% of the regions in this region have a declining trend of eco-environmental quality, mainly concentrated in Qinling Mountains (Figure 5a).

The CCD of Xi'an in this region is better than that of the surrounding cities (Figure 4k–o). Combined with the spatial autocorrelation analysis of CCD in 4.3, although the CCD of Xi'an is higher, the radiation-driving effect of the surrounding cities is weak (Figure 9d–f). At the same time, the current development of tourism in Xi'an promoted regional economic development, but has an impact on the surrounding environment. The phenomenon of negative decoupling of expansion occurred during the period 2015–2017, which has a certain relationship with it.

Therefore, on the one hand, the development of this region should rely on its own ecological and environmental advantages, and develop characteristic industries such as ecological agriculture and tourism through the transformation of ecological resources on the premise of not destroying the ecological environment [64]. On the other hand, it should improve the comprehensive transportation capacity between cities, promote the exchange of economic activities, promote the radiation effect of Xi'an, and promote the coupling and coordinated development of regions [63].

(3) CP and SDP should develop a comprehensive and steady development mode, because the eco-environmental quality, urbanization, and CCD of the CP and SDP showed a higher trend (Figure 5). The regional urbanization level was high, the population density was large, and human activities had a more significant effect on regional eco-environmental protection and coupling and coordination development. From the perspective of municipal and county scales, it can be seen that cities and counties with a higher degree of urbanization have a higher degree of coupling coordination, while regions with a higher quality of ecological environment do not have such a strong corresponding relationship (Figures 4 and 7).

Among them, Zhengzhou in Henan Province and Jinan in Shandong Province have a certain radiation effect on the coupled and coordinated development of surrounding cities (Figure 9d–f), and promoting such radiation effect is more effective for the coupled and coordinated development of the region as a whole.

Therefore, Zhengzhou in Henan Province and Jinan in Shandong Province are taken as two poles to promote cooperation and exchanges between the two urban agglomerations for common development and transition from high-speed growth to high-quality development [63].

6. Conclusions

Based on the GEE platform, Sentinel-2A and other multi-source remote sensing data were used in this study to analyze eco-environmental quality and urbanization and their coupling coordination degree from a multi-scale perspective.

(1) Compared with the RSEI model, the proposed A-RSEI model is more suitable for monitoring the eco-environmental quality of the Yellow River Basin.

(2) From 2013 to 2021, the eco-environmental quality, urbanization, and CCD of the Yellow River Basin are show an increasing trend. In terms of spatial distribution, the performance of the three aspects is slightly different, and the spatial distribution of CCD and urbanization is more similar, showing the characteristics of "high in the east and low in the west". The concentration of CCD increased significantly, and some cities, such as Zhengzhou and Jinan, played a radiating role in driving CCD in the surrounding cities. Most of the cities in the study area are in the ideal decoupling state, the eco-environment has been improved in the process of urbanization development, and the urban development has the characteristics of green and low carbon.

(3) The spatiotemporal characteristics are basically consistent in the Yellow River Basin from urban agglomeration-, municipal-, county-, and pixel-scale perspectives. Specially, the pixel level is better than the municipal-scale in terms of detail, which can be better combined with terrain analysis. The comprehensive discrimination of urban agglomeration and county-scale is helpful to express the relationship between urbanization and eco-environmental quality centered on a certain city.

In the future, we will give more consideration to the impact of human activities on the eco-environment, urbanization, and their coupling coordination degree, such as air pollution, water environment, and land use change.

Author Contributions: Conceptualization, X.W.; methodology, X.W. and S.Z.; software, S.Z. and X.Z.; formal analysis, S.Z.; data curation, S.Z.; writing—original draft preparation, S.Z. and X.Z.; writing—review and editing, S.S. and L.X. All authors have read and agreed to the published version of the manuscript.

Funding: This research was funded by the key scientific and technological project of Henan Province, grant number 212102210137; the Natural Science Foundation of Henan, grant number 212300410292; the key research project of higher Education of Henan Province, China, grant number 21A420006; and the Open Fund of National Engineering Research Center for Geographic Information System, China University of Geosciences, Wuhan 430074, China, grant number 2021KFJJ04.

Data Availability Statement: Not applicable.

Conflicts of Interest: The authors declare no conflict of interest.

References

1. Qiu, M.; Yang, Z.; Zuo, Q.; Wu, Q.; Jiang, L.; Zhang, Z.; Zhang, J. Evaluation on the relevance of regional urbanization and ecological security in the nine provinces along the Yellow River, China. *Ecol. Indic.* **2021**, *132*, 108346. [CrossRef]
2. Fang, C.; Yu, D.J. Urban agglomeration: An evolving concept of an emerging phenomenon. *Landsc. Urban Plan.* **2017**, *162*, 126–136. [CrossRef]
3. Fang, C. Important progress and future direction of studies on China's urban agglomerations. *J. Geogr. Sci.* **2015**, *25*, 1003–1024. [CrossRef]
4. Miao, C.Y.; Yang, L.; Chen, X.H.; Gao, Y. The vegetation cover dynamics (1982–2006) in different erosion regions of the Yellow River Basin, China. *Land Degrad. Dev.* **2012**, *23*, 62–71. [CrossRef]
5. Chen, Y.P.; Fu, B.J.; Zhao, Y.; Wang, K.B.; Zhao, M.M.; Ma, J.F.; Wu, J.H.; Xu, C.; Liu, W.G.; Wang, H. Sustainable development in the Yellow River Basin: Issues and strategies. *J. Clean. Prod.* **2020**, *263*, 121223. [CrossRef]
6. Zhao, Y. Master Planning of Yellow River Basin: Meaning, Measures and Implementing Results. *Yellow River* **2013**, *35*, 5–7.
7. Shao, Z.; Ding, L.; Li, D.; Altan, O.; Huq, E.; Li, C. Exploring the relationship between urbanization and ecological environment using remote sensing images and statistical data: A case study in the Yangtze River Delta, China. *Sustainability* **2020**, *12*, 5620. [CrossRef]
8. Zheng, Z.; Wu, Z.; Chen, Y.; Yang, Z.; Marinello, F. Exploration of eco-environment and urbanization changes in coastal zones: A case study in China over the past 20 years. *Ecol. Indic.* **2020**, *119*, 106847. [CrossRef]
9. Chen, W.; Zhang, Y.; Pengwang, C.; Gao, W. Evaluation of urbanization dynamics and its impacts on surface heat islands: A case study of Beijing, China. *Remote Sens.* **2017**, *9*, 453. [CrossRef]
10. Zhao, M.; Cheng, W.; Zhou, C.; Li, M.; Huang, K.; Wang, N. Assessing spatiotemporal characteristics of urbanization dynamics in Southeast Asia using time series of DMSP/OLS nighttime light data. *Remote Sens.* **2018**, *10*, 47. [CrossRef]
11. Xu, Z.; He, X.; Chen, L.; Hu, X.; Tang, W.; Li, J. How does the urbanization level change in the Yangtze River economic belt, China? A multi-scale evaluation using DMSP/OLS nighttime light data. In *IOP Conference Series: Earth and Environmental Science*; IOP Publishing: Bristol, UK, 2021; Volume 675, p. 012112.
12. Zhou, Y.; Tu, M.; Wang, S.; Liu, W. A novel approach for identifying urban built-up area boundaries using high-resolution remote-sensing data based on the scale effect. *ISPRS Int. J. Geo-Inform.* **2018**, *7*, 135. [CrossRef]
13. Xu, H. A remote sensing index for assessment of regional ecological changes. *China Environ. Sci.* **2013**, *33*, 889–897.
14. Shan, W.; Jin, X.; Ren, J.; Wang, Y.; Xu, Z.; Fan, Y.; Gu, Z.; Hong, C.; Lin, J.; Zhou, Y. Ecological environment quality assessment based on remote sensing data for land consolidation. *J. Clean. Prod.* **2019**, *239*, 118126. [CrossRef]
15. Guo, B.; Fang, Y.; Jin, X.; Zhou, Y. Monitoring the effects of land consolidation on the ecological environmental quality based on remote sensing: A case study of Chaohu Lake Basin, China. *Land Use Policy* **2020**, *95*, 104569. [CrossRef]
16. Xu, H.; Wang, M.; Shi, T.; Guan, H.; Fang, C.; Lin, Z. Prediction of ecological effects of potential population and impervious surface increases using a remote sensing based ecological index (RSEI). *Ecol. Indic.* **2018**, *93*, 730–740. [CrossRef]
17. Zhang, S.; Yang, P.; Xia, J.; Qi, K.; Wang, W.; Cai, W.; Chen, N. Research and analysis of ecological environment quality in the Middle Reaches of the Yangtze River Basin between 2000 and 2019. *Remote Sens.* **2021**, *13*, 4475. [CrossRef]
18. Nie, X.; Hu, Z.; Zhu, Q.; Ruan, M. Research on temporal and spatial resolution and the driving forces of ecological environment quality in coal mining areas considering topographic correction. *Remote Sens.* **2021**, *13*, 2815. [CrossRef]

19. Liu, Z.; Xu, H.; Li, L.; Tang, F.; Lin, Z. Ecological change in the Hangzhou area using the remote sensing based ecological index. *J. Basic Sci. Eng.* **2015**, *23*, 728–739.
20. Pariha, H.; Zan, M.; Alimjan, K. Remote sensing evaluation of ecological environment in Urumqi City and analysis of driving factors. *Arid Zone Res.* **2021**, *38*, 1484–1496.
21. Yue, H.; Liu, Y.; Zhu, R. Monitoring Ecological Environment Chang Based on Remote Sensing Ecological Index in Shendong Mining Area. *Bull. Soil Water Conserv.* **2019**, *39*, 101–107.
22. Hu, S.; Yao, Y.; Fu, J.; Zhao, J.; Hao, D. Evaluation of ecological quality variation in mining area of Northeast China based on RSEI Index: A case study of Gongchangling District, Liaoning. *Chin. J. Ecol.* **2021**, *40*, 4053–4060.
23. An, M.; Xie, P.; He, W.; Wang, B.; Huang, J.; Khanal, R. Spatiotemporal change of ecologic environment quality and human interaction factors in three gorges ecologic economic corridor, based on RSEI. *Ecol. Indic.* **2022**, *141*, 109090. [CrossRef]
24. Yang, X.; Meng, F.; Fu, P.; Zhang, Y.; Liu, Y. Spatiotemporal change and driving factors of the Eco-Environment quality in the Yangtze River Basin from 2001 to 2019. *Ecol. Indic.* **2021**, *131*, 108214. [CrossRef]
25. Wang, J.; Ding, J.; Ge, X.; Qin, S.; Zhang, Z. Assessment of ecological quality in Northwest China (2000–2020) using the Google Earth Engine platform: Climate factors and land use/land cover contribute to ecological quality. *J. Arid Land* **2022**, *14*, 1196–1211. [CrossRef]
26. Wu, S.; Gao, X.; Lei, J.; Zhou, N.; Guo, Z.; Shang, B. Ecological environment quality evaluation of the Sahel region in Africa based on remote sensing ecological index. *J. Arid Land* **2022**, *14*, 14–33. [CrossRef]
27. Li, J.; Li, S.; Guo, W.; Yan, X.; Zhang, R. Ecological Environment Analysis of Shanxi Province and Coal Mining Areas Based on Modified Remote Sensing Ecological Index. *Metal Mine* **2022**. Available online: https://kns.cnki.net/kcms/detail/34.1055.TD.20220907.1435.002.html (accessed on 29 November 2022).
28. DiWu, J.; Mei, J.; Yu, H.; Zhang, Y.; Zhang, Y.X. Construction and Application of Remote Sensing Ecological Index in Semi-arid Region. *Adm. Tech. Environ. Monit.* **2022**, *34*, 21–26.
29. Yang, Y.; Zhang, Y.; Yang, Z. Ecological Analysis of Suzhou City Using Improved Urban Remote Sensing Ecological Index. *J. Geomat. Sci. Technol.* **2021**, *38*, 323–330.
30. Grossman, G.M.; Krueger, A.B. *Environmental Impacts of a North American Free Trade Agreement*; National Bureau of Economic Research: Cambridge, MA, USA, 1991.
31. Shafik, N.; Bandyopadhyay, S. *Economic Growth and Environmental Quality: Time-Series and Cross-Country Evidence*; World Bank Publications: Washington, DC, USA, 1992; Volume 904.
32. Cui, X.; Fang, C.; Li, J.; Liu, H.; Zhang, Q. Progress in dynamic simulation modeling of urbanization and ecological environment coupling. *Prog. Geogr.* **2019**, *38*, 111–125.
33. Gong, Z.; Mao, R.; Jiang, J. Coupling and coordination degree between urbanization and ecological environment in guizhou, China. *Discret. Dyn. Nat. Soc.* **2021**, *2021*, 8436938. [CrossRef]
34. Song, Q.; Zhou, N.; Liu, T.; Siehr, S.A.; Qi, Y. Investigation of a "coupling model" of coordination between low-carbon development and urbanization in China. *Energy Policy* **2018**, *121*, 346–354. [CrossRef]
35. Fang, C.; Cui, X.; Liang, L. Theoretical analysis of urbanization and eco-environment coupling coil and coupler control. *Acta Geogr. Sin.* **2019**, *74*, 2529–2546.
36. Li, W.; Yi, P. Assessment of city sustainability—Coupling coordinated development among economy, society and environment. *J. Clean. Prod.* **2020**, *256*, 120453. [CrossRef]
37. Xie, M.; Wang, J.; Chen, K. Coordinated development analysis of the "resources-environment-ecology-economy-society" complex system in China. *Sustainability* **2016**, *8*, 582. [CrossRef]
38. Shen, L.; Huang, Y.; Huang, Z.; Lou, Y.; Ye, G.; Wong, S.W. Improved coupling analysis on the coordination between socio-economy and carbon emission. *Ecol. Indic.* **2018**, *94*, 357–366. [CrossRef]
39. Fu, S.; Zhuo, H.; Song, H.; Wang, J.; Ren, L. Examination of a coupling coordination relationship between urbanization and the eco-environment: A case study in Qingdao, China. *Environ. Sci. Pollut. Res.* **2020**, *27*, 23981–23993. [CrossRef]
40. He, J.; Wang, S.; Liu, Y.; Ma, H.; Liu, Q. Examining the relationship between urbanization and the eco-environment using a coupling analysis: Case study of Shanghai, China. *Ecol. Indic.* **2017**, *77*, 185–193. [CrossRef]
41. Liu, N.; Liu, C.; Xia, Y.; Da, B. Examining the coordination between urbanization and eco-environment using coupling and spatial analyses: A case study in China. *Ecol. Indic.* **2018**, *93*, 1163–1175. [CrossRef]
42. Zhao, G.; Mu, X.; Wen, Z.; Wang, F.; Gao, P. Soil erosion, conservation, and eco-environment changes in the Loess Plateau of China. *Land Degrad. Dev.* **2013**, *24*, 499–510. [CrossRef]
43. Xu, D.; Cheng, J.; Xu, S.; Geng, J.; Yang, F.; Fang, H.; Xu, J.; Wang, S.; Wang, Y.; Huang, J.; et al. Understanding the Relationship between China's Eco-Environmental Quality and Urbanization Using Multisource Remote Sensing Data. *Remote Sens.* **2022**, *14*, 198. [CrossRef]
44. Framework of Plan for Ecological Protection and High-Quality Development of the Yellow River Basin. Available online: http://www.gov.cn/zhengce/2021-10/08/content_5641438.htm. (accessed on 29 November 2022).
45. Yang, J.; Huang, X. The 30 m annual land cover dataset and its dynamics in China from 1990 to 2019. *Earth Syst. Sci. Data* **2021**, *13*, 3907–3925. [CrossRef]
46. Gong, C.; Wu, W.; Duan, Y.; Liu, H.; He, J.; Sun, C.; Jiang, Q. Evaluation of soil and water conservation function in karst region based on Remote Sensing RMMF Model. *Acta Ecol. Sin.* **2022**, *42*, 4389–4400.

47. Jiao, Z.; Sun, G.; Zhang, A.; Jia, X.; Huang, H.; Yao, Y. Water Benefit-Based Ecological Index for Urban Ecological Environment Quality Assessments. *IEEE J. Sel. Top. Appl. Earth Obs. Remote Sens.* **2021**, *14*, 7557–7569. [CrossRef]
48. Huete, A.; Didan, K.; Miura, T.; Rodriguez, E.P.; Gao, X.; Ferreira, L.G. Overview of the radiometric and biophysical performance of the MODIS vegetation indices. *Remote Sens. Environ.* **2002**, *83*, 195–213. [CrossRef]
49. Shan, Y.; Dai, X.; Li, W.; Yang, Z.; Wang, Y.; Qu, G.; Liu, W.; Ren, J.; Li, C.; Liang, S.; et al. Detecting Spatial-Temporal Changes of Urban Environment Quality by Remote Sensing-Based Ecological Indices: A Case Study in Panzhihua City, Sichuan Province, China. *Remote Sens.* **2022**, *14*, 4137. [CrossRef]
50. Xu, H. A new index for delineating built-up land features in satellite imagery. *Int. J. Remote Sens.* **2008**, *29*, 4269–4276. [CrossRef]
51. Zhang, J.; Yang, G.; Yang, L.; Li, Z.; Gao, M.; Yu, C.; Gong, E.; Long, H.; Hu, H. Dynamic Monitoring of Environmental Quality in the Loess Plateau from 2000 to 2020 Using the Google Earth Engine Platform and the Remote Sensing Ecological Index. *Remote Sens.* **2022**, *14*, 5094. [CrossRef]
52. López-Vicente, M.; Quijano, L.; Palazón, L.; Gaspar, L.; Navas, A. Assessment of soil redistribution at catchment scale by coupling a soil erosion model and a sediment connectivity index (Central Spanish Pre-Pyrenees). *Cuad. Investig. Geogr.* **2015**, *41*, 127–147. [CrossRef]
53. Ouyang, X.; Zhu, X.; He, Q. Spatial interaction betwwen urbanization and ecosystem services: A case study in Changsha-Zhuzhou-Xiangtan urban agglomeration, China. *Acta Ecol. Sin.* **2019**, *39*, 7502–7513.
54. Xu, D.; Yang, F.; Yu, L.; Zhou, Y.; Li, H.; Ma, J.; Huang, J.; Wei, J.; Xu, Y.; Zhang, C.; et al. Quantization of the coupling mechanism between eco-environmental quality and urbanization from multisource remote sensing data. *J. Clean. Prod.* **2021**, *321*, 128948. [CrossRef]
55. Zheng, H.; Khan, Y.A.; Abbas, S.Z. Exploration on the coordinated development of urbanization and the eco-environmental system in central China. *Environ. Res.* **2022**, *204*, 112097. [CrossRef]
56. Petri, T. Towards a theory of decoupling: Degrees of decoupling in the EU and the case of road traffic in Finland between 1970 and 2001. *Transp. Policy* **2005**, *12*, 137–151.
57. Li, T.; Wang, J.; Zhang, G.; Cui, Y.; Yao, Z. Spatiotemporal characteristics of an ecological footprint, decoupling effect tendency, and grey prediction in Hefei City. *Acta Ecol. Sin.* **2019**, *39*, 1735–1747.
58. Xiang, K.; Zhao, A.; Liu, H.; Zhang, X.; Zhang, A.; Tian, X.; Jin, Z. Spatiotemporal Evolution and Coupling Pattern Analysis of Urbanization and Ecological Environmental Quality of the Chinese Loess Plateau. *Sustainability* **2022**, *14*, 7236. [CrossRef]
59. Yang, Z.; Tian, J.; Su, W.; Wu, J.; Liu, J.; Liu, W.; Guo, R. Analysis of Ecological Environmental Quality Change in the Yellow River Basin Using the Remote-Sensing-Based Ecological Index. *Sustainability* **2022**, *14*, 10726. [CrossRef]
60. Chen, S.; Huo, A.; Zhang, D.; Chen, S.B.; Zhao, Z.; Chen, J. Key technologies for drought disaster risk assessmentin typical vulnerableareas of eastern Gansu Province. *Agric. Res. Arid Areas* **2022**, *40*, 197–204.
61. Lu, G.; Pang, X.; Hou, J.; Hao, J. Evaluation and prediction of ecological security in Shizuishan City based onPSR model. *J. Saf. Environ.* **2023**. [CrossRef]
62. Wang, L.; Feng, C. Evolutionary Mechanism and Development Strategy of Resoure-based City: Taking Gansu Baiyin as An Example. *Areal Res. Dev.* **2013**, *32*, 65–70.
63. Zhang, L.; Wu, M.; Bai, W.; Jin, Y.; Yu, M.; Ren, J. Measuring coupling coordination between urban economic development and air quality based on the Fuzzy BWM and improved CCD model. *Sustain. Cities Soc.* **2021**, *75*, 103283. [CrossRef]
64. Chen, Y.; Zhang, D. Multiscale assessment of the coupling coordination between innovation and economic development in resource-based cities: A case study of Northeast China. *J. Clean. Prod.* **2021**, *318*, 128597. [CrossRef]